Applied Mathematics and Information Sciences
An International Journal

Detecting Retinal Damage with Image Analysis using Machine learning Algorithm

Anitha. E[1,2,*] *and A. Antonidoss* [1]

[1]Computer Science and Engineering, Hindustan Institute of Technology and Science, Padur, Chennai, India
[2]Information Technology, Loyola-ICAM College of Engineering and Technology, Nungambakkam, Chennai, India

Abstract: Retina is an important layer of tissue in the back of the eye. The retina's primary job is to gather light that the lens has focused, convert the light into neural signals, and send those signals to the brain for optical compensation. This crucial tissue may appear damaged due to retinal detachment (RD). Such conditions can impair vision and undoubtedly have the potential to be severe enough to cause blindness. It can be challenging to identify the damage since the layers and the nerve connections are too delicate and thin, and they may be mistaken for another illness. IMRCNN, an improved mask recurrent convolutional neural network, was proposed to test its efficiency in RD detection. The effectiveness of the suggested approach is evaluated by looking at the implementation measures Sensitivity (S), Accuracy (A), Specificity (SP), and F-score (F). For 54,000 retinographic images, the average S, SP, A, and F values were 92.20%, 98%, 95.10%, and 93%, respectively. This suggested model performs better at classifying RD-related lesions and classifying the intensity levels on various retinal pictures. This type of analysis methodology concentrates on breaking down images into pixels and studying the data from the bottom up. It offers greater analysis and more precisely detects RD. This study presents essential knowledge and cutting-edge machine learning methodologies in the field of medical image processing methods and analysis. The main objectives of this work are to define and apply the identified and addressed important principles as well as to provide research on medical image processing.

Keywords: Retinal detachment, Improved mask recurrent convolutional neural network, Retinographic images, Medical image processing

1 Introduction

The retina is the membrane of sensory receptors within the internal surfaces of the eyeball's posterior portion. Several layers of cells, including these specialized cells known as photoreceptors, are utilized in the formation of the retina. There are two categories of photoreceptors in the human eye rods and cones [1]. The rod photoreceptors discover signals, offer black-and-white perception, and perform effectively in little illumination. Cones are important for trichromacy and visible pleasure and accomplish well in standard and brilliant lighting. As rods are inserted in the retina, cones are focused on the macula, a small, central region of the retina. The fovea, or minor depression found in the macula, can be found at its center shown in Figure 1. The fovea is the part of the retina with the highest density of cone photoreceptors and is responsible for maximum sharp-sightedness and vision [2].

Retina Functions: Photoreceptor cells sense intense mild emitted from the cornea and lens. It then converts that mild into chemical and frightened indicators that are transported to the brain through nerve optics. They are transformed into pixels and visible impressions when they reach the cortical region of the brain [3].

Retina Problems:

1. Macular degeneration - an illness that abolishes your acute and vital vision
2. Diabetic eye infection
3. Retinal objectivity - a medical substitute, when the retina is hauled aside from the following of the eye
4. Retinoblastoma - cancer of the retina. It is an utmost joint in young youngsters.
5. Macular pucker - scar tissue on the macula

---

* Corresponding author e-mail: esanitha.me@gmail.com
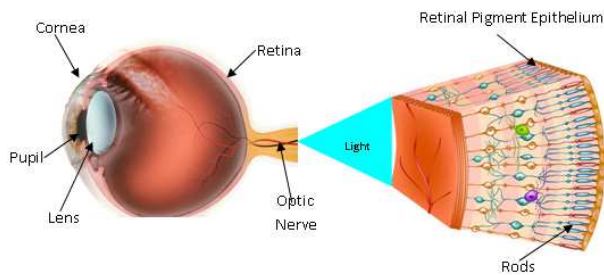
Fig. 1: Image of Retinal Damage

6. Macular hole - a lesser disruption in the macula that typically occurs in people at the end of 60
7. Floaters - cobwebs or specks in your enclosure of vision

The above issues have been addressed by developing a new technique for predicting & classifying retinal images. This method helps to mitigate the problem of vision loss caused by RD.To obtain an exact identification of RD, many studies have proposed various approaches. Curvelet equations obtained from endoscopies and retinal images are frequently applied. The experiment was performed on 70 diabetics and a three-step classification method was used [4]. Consequently, the predicted technique attains a sensitivity value of 100%. A method for the classification of RD images treated according to previous micro aneurysms has been introduced [5]. In addition, the circularity and location of the microaneurysm were used in the feature extraction process.

Using filters, 3 techniques for segments and sub-anterior detection were used.All potential areas in the retinal image were identified in the initial system phase [6]. A mixed classification structure consisting of a variation model and a vector machine was then used to classify these locations.According to a 2013 statement [7], the approach can recognize spherical or somewhat expanded image forms and can differentiate vascular branch points and conversions. A method for determining diabetes from the fundus of the retinal eye focused on an automated system that was designed to quickly and accurately categorize vision loss.

2 Related Work

In an earlier study, an RD phase grouping existed using 80,000 images from the Kaggle machine learning principles in response to Convolutional Neural Network (CNN) networks' exceptional performance in RD diagnosis. To categorize the class five severity levels of RD, it developed the CNN design with the information intensification & recognized complex RD structures as Hemorrhage (HEM), & diffusion on the retina [8]. On

validation data from 5,000 data points, studies using a premium graphics processor produced A and Sresults of 75% and 95%, respectively.With the help of 54 registered optometrists, CNN ranked multiple stages of RD on 128,000 background photos [9]. In RD stage classification, both CNN prototypes completed an SP of 93.9% and an S of 97.5%. The goal of the research is to generate a deep learning system that automatically chooses the most useful patches and photos for creating workable masks and RD grading for predicting RD-related areas for significance [10]. Owing to its strong perspective for learning structures from a small number of learning illustrations relative to the entire dataset, an Active Deep Learning (ADL) strategy is used for this purpose [11]. With the help of the potent machine learning technique known as ADL learning, a training procedure can attain great precision with little to no learning data. It is currently the best method for creating more accurate Computer Aided Diagnosis (CAD) systems and creating affordable medical datasets in situations where expert labeling is expensive and time-consuming. The notion of computer vision encompasses a subset of Artificial Intelligence (AI) that allows electronic systems to gather information from multimedia files including images, videos, and other visual data [12].
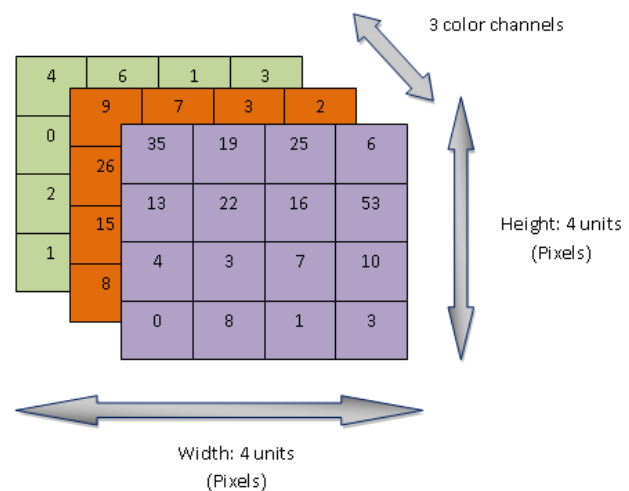

Fig. 2: Image representation in computer vision

Utilizing computer vision combined with mathematical modeling on medical images such as Retinal Optical Coherence Tomography (OCT) images can provide greater insight into retinal damage and help detect retinal damage with greater precision shown in Figure 2. Typically, Radiologists are required to conduct similar tasks, such as identifying patterns of irregularity in medical image data. Consequently, computer vision is the best choice to assist the radiologist in performing

some of the tasks, thus enhancing productivity. Types of Medical Imaging Algorithms include:

Classification: Using this algorithm, the given image will be classified into two or more categories.

Segmentation: The term refers to a technique for encoding a series of pixels in an image that represents the portion of a pattern that has been detected. Often, this determines the size of the abnormality. By comparing images taken at different times, see how the abnormality changes in size.

Localization: Localization refers to the process by which an algorithm can identify the location of a problematic pattern by drawing a bounding box around it.

Outcomes of Computer Vision in Medical Imaging

Diagnostic Assistance: Radiologists often examine several images each day. The radiologist can benefit from the application of AI algorithms to save time spent diagnosing by highlighting suspicious areas of the image or numerically quantifying the area under suspicion.

Screening and Triaging: If there is a long queue of images to be reviewed by a Radiologist, an AI algorithm can be applied to analyze and triage the images in the Picture Archiving and Communication System(PACS), so that the most essential instances receive prompt attention.

Monitoring: To analyze the response to a particular treatment (e.g. in Oncology), photographs of diseased tissues are aligned and compared in distinctive instances. Extrusion in the length of diseased tissue may assist in determining the response to treatment.

Charting: Following a medical review of findings made by the AI tool by a medical professional, such a typical AI product will provide the necessary inputs for clinical charting that would normally have to be entered manually.

3 Proposed System

The strategy proposed in this work is an appropriate response to the need for methods that combine strong computing load with a deductive approach to enhance the classification precision of retinal fundus images. The optometrist scales each specimen from 0 to 4 for each RD class [13]. The normal condition is represented by a level of 0, while the mild, medium, acute, and proliferative RD are shown by scores of 1, 2, 3, and 4, respectively. And these scales serve as tags in the proposed IMRCNN. The level of visual quality is not standardized. The range of lighting, color averages and aspect ratios are all included in each image, as well as odd lighting and an extra black limit. These retinal samples harm the classifying & division capabilities of RD-based CAD methods. Used 54000 retinal OCT images from an online healthcare repository from the repository http://www.cell.com/cell/fulltext/S0092-8674(18)30154-5.

3.1 Visual representation of the input data

The data file has images from four classes shown in Figures 3 to 6 which are as follows.

1. Choroidal Neovascularization (CNV) - label 1
2. Diabetic Macular Edema (DME) - label 2
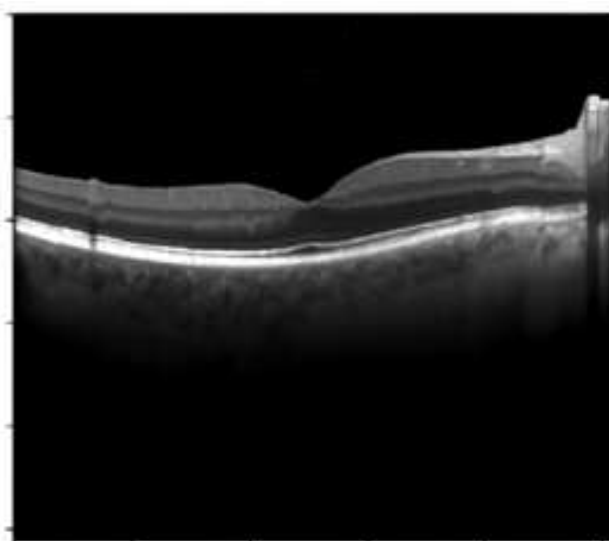3. Multiple drusen (drusen) - label 3
4. Healthy (normal images) - label 0

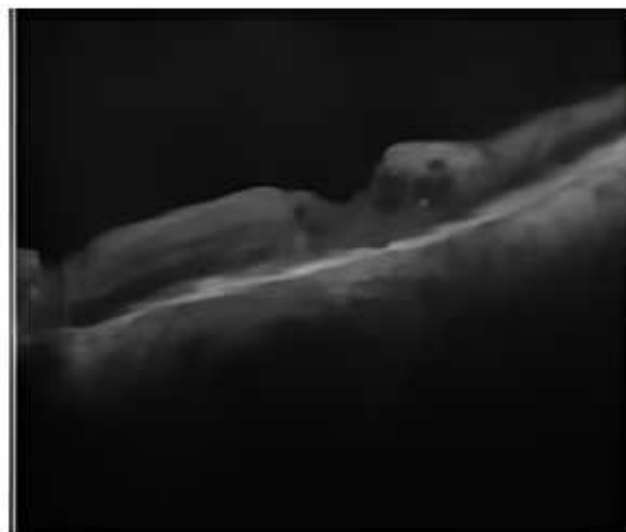

Fig. 3: Normal retina

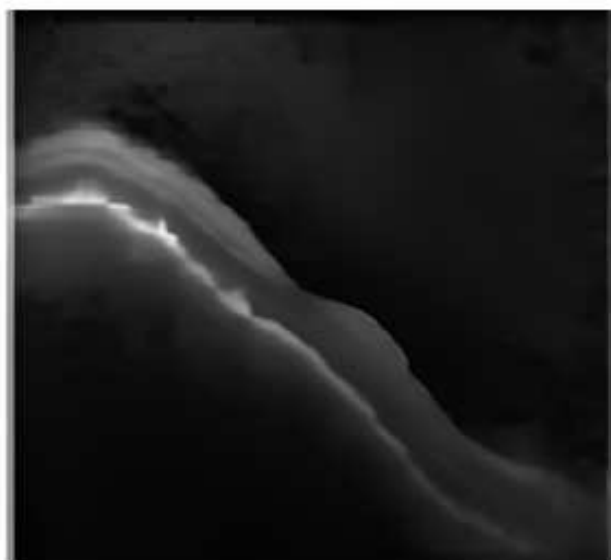
Fig. 4: CNV

Fig. 5: DME

Fig. 6: Drusen

3.2 Data preprocessing

Data is preprocessed and a random lighting scheme is applied to enhance the image to enhance the features. Then, the data is converted to tensor units with vector attributes in 2D space, along with other attributes, such as shape, size, and angle.

Following this, the particular is prepared for learning and the rest is set aside for assessment.

Train size = 756

Test size = 208
Train data shape = 792 x (150, 150,3)

3.3 Improved Mask Recurrent Convolutional Neural Network(IMRCNN)

IMRCNN consists of a set of rules that incorporates Deep Learning rules whatever may be receipt in a given image and allocate reputation (learnable masses and preferences) to several factors/components within the image, and be able to distinguish one from the other. Numerous components make up the structure. IMRCNN is the most important component. It carries out import operations.

Convoluting is the first operation, so max pooling follows. These operations enable one to extract more potent and specific functions from the image of a man or woman. Additionally, these functions are hired through hidden layers of the deep community that adjust the weights by the jobs shown in Figure 7.
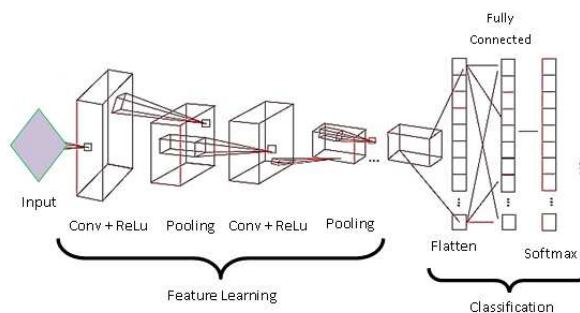

Fig. 7: Flow of IMRCNN

Consequently, the deep layer is hidden, and as a result, the schooling takes place after the functions are flattened from a multidimensional tensor to a vector, in line with the illustration.

Rectified Linear Unit (ReLU): In a neural community, activation influences the remodeling of the aggregate stacked inputs from the nodes into stimulation of the nodes or results associated with those inputs. It could be considered a piecewise linear function that results in the given data instantly if it is affirmative, then it will result in nil. A model that uses it has developed the avoidance activation function for numerous different kinds of neural networks shown in Figure 8. This is in part because it is accessible to coaches and sometimes outcomes in enhanced enactment.

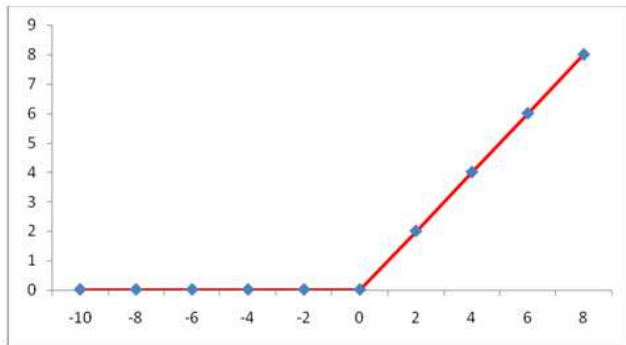Equation of Relu:

$$y = \max(0, x)$$

Fig. 8: Representation of ReLu

3.4 Softmax Function

The softmax function is employed because the activation functions within the resulting level of neural network simulations forecast a multinomial probability distribution. Certain, softmax is employed because the activation functions for multi-class cataloging complications wherever class affiliation is essential on quite two class labels shown in Figure 9.

Fig. 9: Representation of softmax transformation

IMRCNN transforms the input photo in a way that allows capabilities to be extracted from it. A kernel (or clear out) is convolved with the image in this transformation. A kernel is a lesser matrix whose width and altitude are lesser than the photo to be contortion. It is also known as a convolution matrix or convolution mask.

This enables the extraction of capabilities through filtering photographs in extraordinary approaches along with lines, curves, rows, angles, lighting, and form. Each convolution layer is doubled on this architecture Max pooling. The pooling operation involves sliding a two-dimensional clear-out over every channel of the function map and summing up the capabilities mendacity

Layer (type)	Output Shape	Param #
input_1 (InputLayer)	(None, 150, 150, 3)	0
block1_conv1 (Conv2D)	(None, 150, 150, 64)	1792
block1_conv2 (Conv2D)	(None, 150, 150, 64)	36928
block1_pool (MaxPooling2D)	(None, 75, 75, 64)	0
block2_conv1 (Conv2D)	(None, 75, 75, 128)	73856
block2_conv2 (Conv2D)	(None, 75, 75, 128)	147584
block2_pool (MaxPooling2D)	(None, 37, 37, 128)	0
block3_conv1 (Conv2D)	(None, 37, 37, 256)	295168
block3_conv2 (Conv2D)	(None, 37, 37, 256)	590080
block3_conv3 (Conv2D)	(None, 37, 37, 256)	590080
block3_pool (MaxPooling2D)	(None, 18, 18, 256)	0
block4_conv1 (Conv2D)	(None, 18, 18, 512)	1180160
block4_conv2 (Conv2D)	(None, 18, 18, 512)	2359808
block4_conv3 (Conv2D)	(None, 18, 18, 512)	2359808
block4_pool (MaxPooling2D)	(None, 9, 9, 512)	0
block5_conv1 (Conv2D)	(None, 9, 9, 512)	2359808
block5_conv2 (Conv2D)	(None, 9, 9, 512)	2359808
block5_conv3 (Conv2D)	(None, 9, 9, 512)	2359808
block5_pool (MaxPooling2D)	(None, 4, 4, 512)	0
flatten_1 (Flatten)	(None, 8192)	0
dense_1 (Dense)	(None, 4)	32772

Fig. 10: Architectures building blocks

in the location covered by the clear-out shown in Figure 11.

4 Results and Discussions

4.1 Training

This method of resampling is used to assess device learning patterns on a restricted sample of data shown in Figure 12.

Feature vectors of train samples were trained with 756 train samples and 168 validated samples over 12 epochs. In every case, the data is shifted and blocks of data are used for confirmation and training shown in Figure 13 Each step is validated and updated for accuracy. Every step of the training involves an adjustment of the network's weights
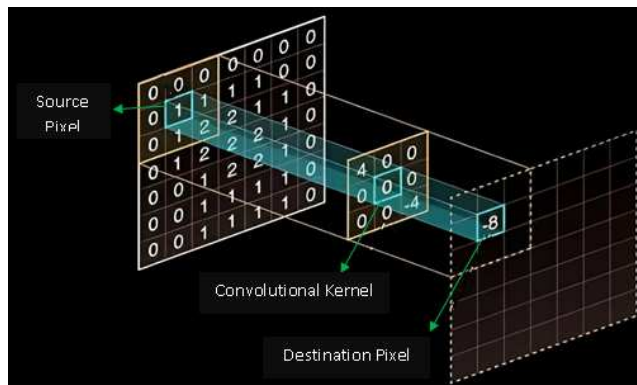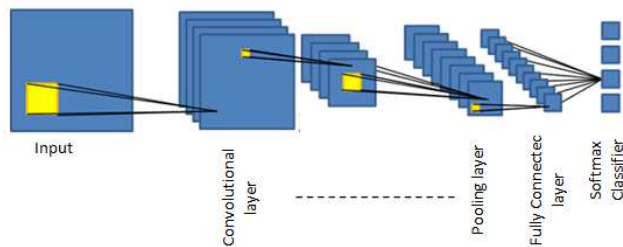
Fig. 11: IMRCNN Process

Fig. 12: Training steps

Fig. 14: Accuracy and loss

shown in Figure 14 (a) and (b). The weights serve to tune the model to the specifics of the data, which allows it to make the prediction or detection task much more accurate.
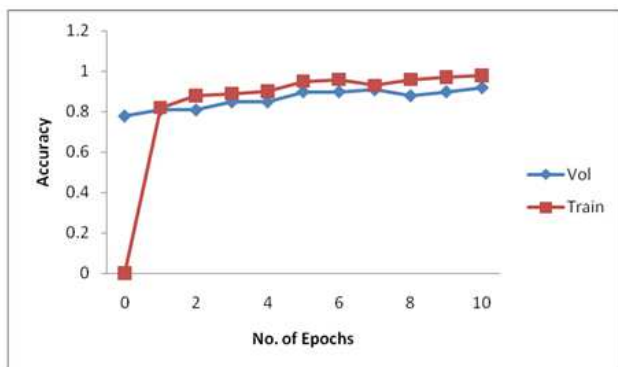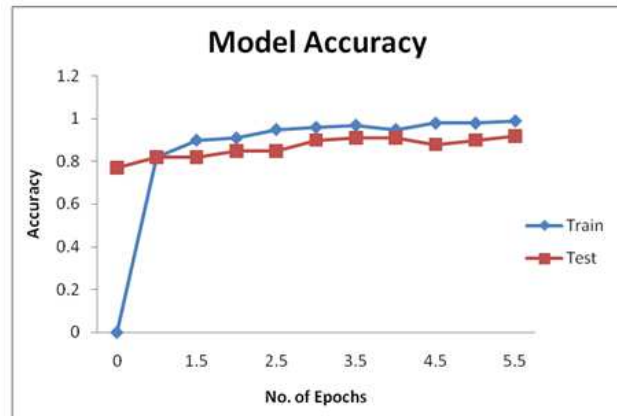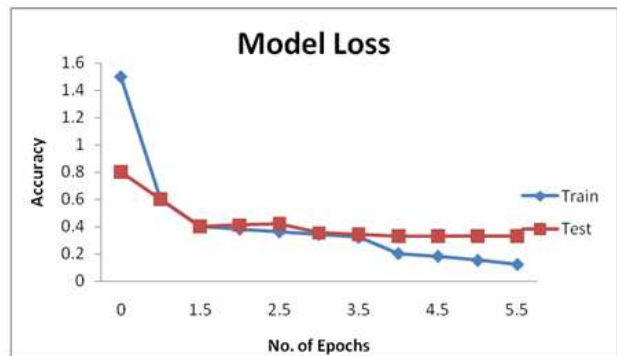
coherent, the model would be an excellent baseline model for the classification of retinal images.

4.2 Model improvisation: Fine Tuning

After the baseline model has been developed, the model is fine-tuned to fit the data in Figure 15. The fine-tuning process involves changing the hyperparameters and using the appropriate number of epochs to avoid over- or under-fitting shown in Figures 16 (a) and (b).

Fig. 13: Train vs Test

4.3 Evaluation metrics

Based on the evaluation metrics, it can be concluded that the fine-tuned model has a good fit since it produces accurate outcomes with low bias and variance explained in Table 1.
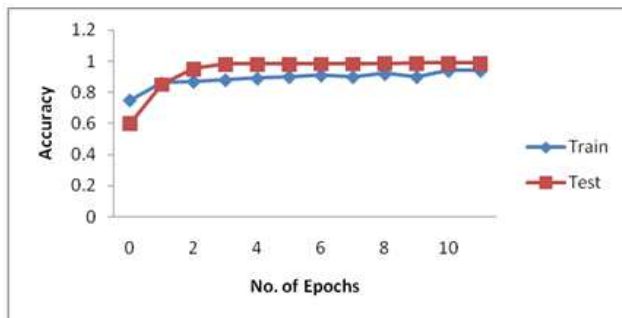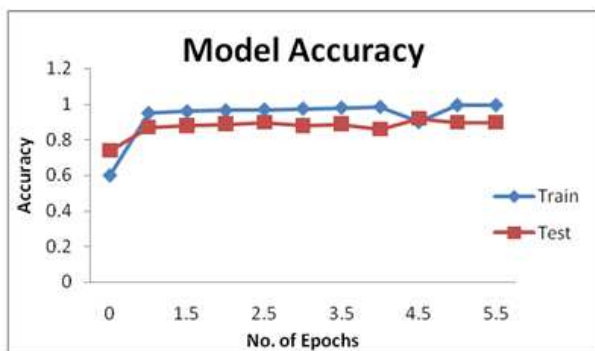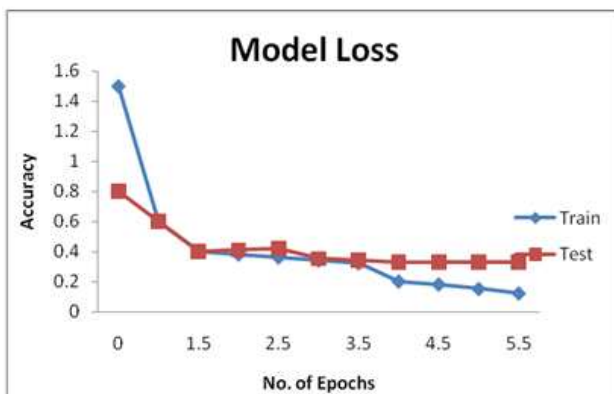
In training, the accuracy is 98.81%, whereas in testing it is 91.67%. Since the variance between these two lines is

Fig. 15: Fine-tuned model

Table 1: Fine-tuned result

Parameters	SP	A	F	S
Normal	0.9	0.9	0.9	0.9
CNV	0.94	0.98	0.95	0.95
DME	0.92	0.86	0.89	0.86
DRUSEN	0.03	0.95	0.94	0.84
avg/total	0.92	0.92	0.92	0.88

training of the IMRCNN model proposed in the experiment. The initial ADL-formation of CNN is finished when the orange line becomes solid. It selects the most relevant image before updating the network settings. With this approach, the performance measures are shown in Figure 17 (a) – (c). It demonstrates even more how effective our training method is in comparison to other common techniques for building CNN models. The confusion matrix is explained in Table 2.

4.5 Confusion matrix

Table 2: Confusion Matrix

	Confusion matrix			
	Param	Normal	CNV	DME	DRUSEN
True	Normal	39	0	4	1
	CNV	0	42	0	1
	DME	4	3	37	1
	DRUSEN	1	1	0	42
	Predicted			

Upon completion of the first simulation, a portion of the image sequence was determined by summing all of its EGL values. It outlines the standards for choosing photos for algorithm outputs. As the network investigated other batches, this value was plotted and analyzed, as shown in Figure 18. The reduction in attribute value after model completion was observed in this case. This indicates that the loss feature will not continue to decline and that the variable standard is very close to 0.

(a)

(b)

Fig. 16: Fine-tuned - accuracy, and loss
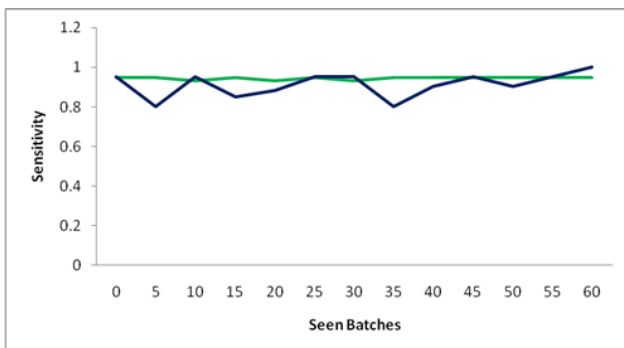
4.4 Model evaluation

As opposed to patching, expert ophthalmology selects the most relevant retinographic samples for labeling and
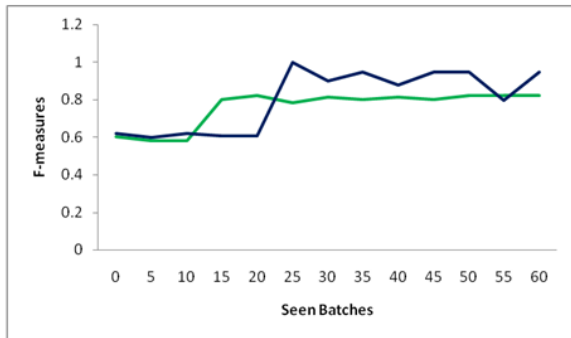
(a)

(b)

(c)

Fig. 17: IMRCNN model result analysis based on performance measures

On 54,000 digitized retinal specimens, a data test based on F, S, SP, & A was performed to determine how well the IMRCNN system performed in categorizing every NPDR class for RD diagnosis.
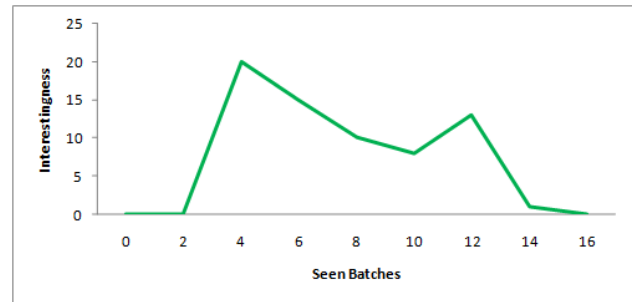

Fig. 18: IMRCNN model result analysis based on performance measures

5 Conclusion

Due to the complex architecture & varying looks of the lesions within the fundus image, it is difficult to distinguish between the five severities of RD utilizing a fundus images image. The majority of research in the literature uses only the RD class, with extremely important findings. In opposition to using the entire collection of training examples, our study has demonstrated the 7-layered architecture utilizing an IMRCNN that automatically & synchronously recognizes the 5 phases of the RD with the determination of abrasions utilizing particular broken-up annotation retina specimens. Before being introduced into the model to learn the distinguishing features, an input wallpaper image was the major pre-processed to develop divergence in the reinforcement approaches and uniform color space.

References

[1] J.-S. Li, Y.-F. Zhang, and Y. Tian, Medical Big Data Analysis in Hospital Information System, *Big Data on Real-World Applications*, (2016).

[2] M. S. Islam, M. M. Hasan, X. Wang, H.D Germack and Noor-E-Alam M, A Systematic Review on Healthcare Analytics: Application and Theoretical Perspective of Data Mining, *Healthcare (Basel)*, **6**(2),54 (2018).

[3] Mohammad Alkhatib and Amir Talaei-Khoei and Amir Hossein Ghapanchi, Analysis of Research in Healthcare Data Analytics, (2016).

[4] S. H. Adil, M. Ebrahim, K. Raza, S. S. Azhar Ali and M. Ahmed Hashmani, *Liver Patient Classification using Logistic Regression*, 2018 4th International Conference on Computer and Information Sciences (ICCOINS), Kuala Lumpur, Malaysia, 1-5, (2018).

[5] B. Vijayakumari and M. Manikumaran, *Pathological lung classification using random forest classifier*, 2017 International Conference on Intelligent Computing and Control (I2C2), Coimbatore, India, 1-5, (2017).

[6] Pooja.V. Magdum and Mahadev.S.Patil, *Comparison of Different Convolutional Neural Network Structures Based on Keras*, (2020).

[7] Zeng, Xianglong et al., Automated Diabetic Retinopathy Detection Based on Binocular Siamese-Like Convolutional Neural Network, *IEEE Access*, **7**, 30744-30753, (2019).

[8] Liu, Xiaoming et al., Semi-Supervised Automatic Segmentation of Layer and Fluid Region in Retinal Optical Coherence Tomography Images Using Adversarial Learning, *IEEE Access* , **7**, 3046-3061, (2019).

[9] Y. Shen, L. Xiao, J. Chen and D. Pan, A Spectral-Spatial Domain-Specific Convolutional Deep Extreme Learning Machine for Supervised Hyperspectral Image Classification, *IEEE Access7*, **7**, 132240-132252, (2019).

[10] Adal KM, van Etten PG, Martinez JP, Rouwen KW, Vermeer KA and van Vliet LJ, An Automated System for the Detection and Classification of Retinal Changes Due to Red Lesions in Longitudinal Fundus Images, *IEEE Trans Biomed Eng*, **65**(6), 1382-1390 (2018).

[11] W. Cao, N. Czarnek, J. Shan and L. Li, Microaneurysm Detection Using Principal Component Analysis and Machine Learning Methods, *IEEE Transactions on Nano Bioscience*, **17**(3), 191-198,(2018).

[12] Hanqing Sun , Zheng Liu , Guizhi Wang, Weimin Lian and Jun Ma, Intelligent analysis of medical big data based on deep learning, (2019).

[13] Ajay Shrestha and Ausif Mohmood, Review of Deep learning algorithms and architectures, *IEEE*, **7**, 53040-53065,(2019).

[14] Flaxman, Seth R., et al., Global causes of blindness and distance vision impairment 1990-2020: a systematic review and meta-analysis, *The Lancet Global Health*, **5**(12), (2017).

[15] K. He, X. Zhang, S. Ren, and J. Sun, *Deep residual learning for image recognition*, in Proceedings of the IEEE conference on computer vision and pattern recognition, 770–778, (2016).

[16] D. Lu, M. Heisler, S. Lee, G. W. Ding, E. Navajas, M. V. Sarunic and M. F. Beg, Deep-learning based multiclass retinal fluid segmentation and detection in optical coherence tomography images using a fully convolutional neural network, *Medical image analysis*, **54**,100-110, (2019).

[17] A. Krizhevsky, I. Sutskever, and G. E. Hinton, Imagenet classification with deep convolutional neural networks, *Advances in neural information processing systems*, 10971105, (2012).

[18] S. H. Kang, H. S. Park, J. Jang, and K. Jeon, Deep neural networks for the detection and segmentation of the retinal fluid in oct images, *MICCAI Retinal OCT Fluid Challenge (RETOUCH)*, (2017).

[19] L. Bekalo, S. Niu, X. He, P. Li, I. P. Okuwobi, C. Yu, W. Fan, S. Yuan, and Q. Chen, Automated 3-d retinal layer segmentation from sd-oct images with neurosensory retinal detachment, *IEEE Access*, **7**,14894– 14907, (2019).

[20] X. Li, L. Shen, M. Shen, and C. S. Qiu, Integrating handcrafted and deep features for optical coherence tomography based retinal disease classification, *IEEE Access*,**7**,33771–33777, (2019).

Anitha E, has completed her Master's in Computer science and Engineering and currently working as an assistant professor at Loyola- ICAM College of Engineering and Technology. She has 9 years of teaching experience. She is currently pursuing her PhD in Machine learning at Hindustan Institute of Technology and Science. Her areas of interests include Web services, Network security and Machine Learning.

A. Antonidoss B.E., M.E., Ph.D, currently working as Associate Professor in Hindustan Institute of Technology and Science, Chennai. He has published 26 research works with 43 citations and 686 reads. His area of interest Cloud Computing, database, Big data analytics, Network analysis, Machine Learning and Block chain.